Affordable Evaluation of 5G Modulation Schemes in High Speed Train Scenarios

José Rodríguez-Piñeiro, Tomás Domínguez-Bolaño, Pedro Suárez-Casal, José A. García-Naya, and Luis Castedo
University of A Coruña, A Coruña, Spain
{j.rpineiro, tomas.bolano, pedro.scasal, jagarcia, luis}@udc.es

***Abstract*—The radio access technology for railway communications is expected to migrate from GSM for Railways (GSM-R) to fourth generation (4G). Recently, considerable attention has been devoted to high-speed trains since this particular environment poses challenging problems in terms of performance simulation and measurement. In order to considerably decrease the cost and complexity of high-speed measurement campaigns, we have proposed a technique to induce effects caused by highly-time varying channels on Orthogonal Frequency-Division Multiplexing (OFDM) signals while conducting measurements at low speeds. This technique has been proved to provide accurate results both for the cases of WiMAX and Long Term Evolution (LTE) signals. In this work, we illustrate the performance of this technique by employing the modulation techniques which are being proposed for fifth generation (5G) systems. More specifically, we compare the results of Filter Bank Multicarrier (FBMC) signals evaluated at different velocities by means of simulations and considering two prototype filters as well as the rural area and typical urban channel models standardized by the 3rd Generation Partnership Project (3GPP).**

I. Introduction

Over the last few years, broadband communication between nodes moving at high speeds has attracted a lot of attention. One of the most relevant research topics in this field is the High-Speed Train (HST) channel modeling. Nowadays, the most widely used communication system between trains and the elements involved in operation, control, and intercommunication of the railway infrastructure is based on the Global System for Mobile Communications (GSM). This technology, namely the GSM for Railways (GSM-R), is not well-suited for supporting advanced services such as automatic pilot applications or provisioning broadband services to the train staff and passengers. Next to trains, the increasing number of broadband services available for mobile devices motivated the migration from the third generation (3G) mobile networks to the fourth generation (4G) ones, mainly Long Term Evolution (LTE), while the fifth generation (5G) mobile networks are currently being defined. Therefore, 5G systems seem to be good candidates to substitute the GSM-R as the basis technology for railway communications in the long term.

One of the most remarkable proposals for the definition of 5G is the utilization of Filter Bank Multicarrier (FBMC) modulation techniques instead of the well-known Orthogonal Frequency-Division Multiplexing (OFDM). In the ensuing paragraphs we emphasize the most important advantages offered by FBMC with respect to OFDM for the railway environment.

- FBMC offers a higher bandwidth efficiency, which is very beneficial as the simultaneous communications between different trains can be more efficiently allocated into the scarce spectrum available in railway environments.
- Co-existence between the current GSM-R and the new broadband systems is a major concern in railway industry. OFDM-based systems usually exhibit a high co-channel interference, leading to a potential performance impact on current GSM-R systems. FBMC-based systems are much more efficient in this sense, thus allowing for better co-existence with current systems such as GSM-R.
- While Multiple Access OFDM (OFDMA) is adequate for efficiently allocating a subset of subcarriers per user in the downlink, the situation is different in the uplink because the users' signals must arrive at the Evolved NodeB (eNodeB) synchronously, both in terms of symbol timing and carrier frequency. For a practical deployment, a close-to-perfect carrier synchronization is necessary [1], which is affordable in a stationary network, but becomes a very difficult task –if not impossible– in a network including mobile nodes. Morelli et al. [2] studied this in detail and concluded that the best way of facing this problem is through the use of a bank of filters to separate the users. However, due to the use of close-to-perfect subcarrier filters, FBMC avoids multiple-access interference without requiring sophisticated synchronization methods, since the subcarriers are well frequency-localized.
- Finally, one of the most important differences between OFDM and FBMC waveforms is their behavior under doubly dispersive channels, like the ones present in HST communications. In this case, the design of the prototype filter must achieve a compromise between the channel response spreading in time (multipath effect) and in frequency (due to the Doppler shift in different multipaths) [1]. In this sense, since OFDM is defined by means of a rectangular window in time, each OFDM symbol appears unbounded in the frequency domain, hence becoming a poor choice for doubly selective channels. According to several studies (see [3]–[7]), FBMC waveforms perform much better for doubly selective channels with respect to OFDM because such prototype filters can be designed specifically for minimizing both time and frequency dispersion.

In previous works (e.g., [8], [9]) we mentioned the most relevant channel models for moving radio interfaces, including the HST environment. We also motivated the need of experimental evaluations for better characterizing the HST environment. However, to the best of our knowledge, no practical evaluation of FBMC techniques in the HST environment is available up to now. One of the reasons that explains the small number of measurement campaigns in high-speed environments is their complexity, cost, and safety constraints[1]. Furthermore, it is not possible, in most cases, to measure at high speeds in controlled environments in a reproducible and repeatable way. In addition, measuring in HST environments demands for specific hardware and software solutions (see, e.g., [10]). In order to address those problems we proposed a technique to induce the effects caused by highly time-varying channels in OFDM signals while conducting the measurements at much lower speeds [11]. This technique consists basically in reducing the subcarrier spacing of the OFDM signal by scaling down the bandwidth of the whole OFDM signal. More specifically, we propose to interpolate the transmit OFDM signal in the time domain before being transmitted. The time-interpolated signal conveys exactly the same information as the original one but with a reduced subcarrier spacing, thus artificially increasing the sensitivity to the Inter-Carrier Interference (ICI). For example, if we time-interpolate the transmit OFDM signal by a factor I, the subcarrier spacing will be reduced by the same factor I, which is similar to what would happen if transmissions were conducted at I times the original speed.

Whereas in [11] and [12] we considered the transmission of standard-compliant WiMAX Mobile (IEEE 802.16e) signals, in [8] and [9] standard-compliant LTE signals were used. In this work, we consider the transmission of FBMC signals. We perform the validation of our technique for FBMC waveforms by means of simulations, considering transmissions at high speeds in both rural and urban environments. The obtained results show that the proposed technique induces highly time-varying channels with excellent agreement for FBMC signals, thus it can be used for dramatically reducing the cost of experimental evaluations for future 5G communications systems in HST scenarios.

II. Emulating High Speeds by Time Interpolation

Let us consider an FBMC modulation where N_c subcarriers are multiplexed to construct each FBMC symbol. Each FBMC symbol has a total length of N_t samples that are transmitted at a rate $F_s = 1/T_s$. Therefore, each FBMC symbol has a time duration $T_t = T_s N_t$. When an FBMC signal is transmitted, the received signal, namely $r(n)$, can be represented in discrete time as

$$r(n) = \sum_{\tau} h(n,\tau) * s(n-\tau) + w(n), \qquad (1)$$

[1]Measuring at typical high speed train velocities requires safety measurements which are not necessary if such measurements are conducted at much lower speeds.

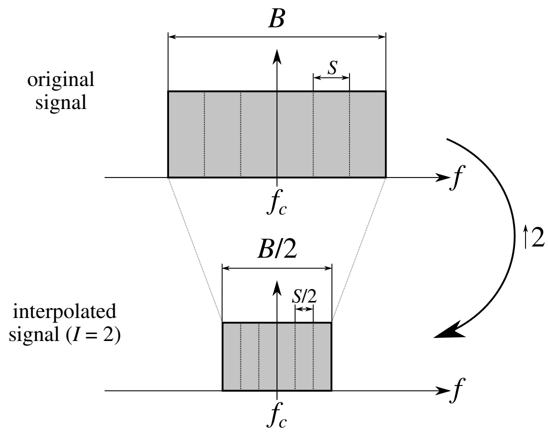

Fig. 1. Example of spectrum compression due to a time interpolation factor $I = 2$. It is straightforward to see that the subcarrier spacing S is also reduced by a factor of I since the total bandwidth B is also reduced by the same factor.

where $x(n)$ contains the transmitted FBMC signal, $h(n,\tau)$ is the discrete-time channel impulse response, $w(n)$ corresponds to uncorrelated complex-valued white Gaussian noise with variance σ_w^2, and $*$ denotes the convolution operation. Note that the statistical properties of the noise are not changed by the decimation process regardless of the interpolation factor.

When multicarrier systems are used in time-selective channels, ICI arises in the received signal. The amount of ICI relates to the normalized Doppler spread of the channel, which is given by $D_n = f_d T$, f_d being the maximum Doppler frequency and T the FBMC symbol period, which depends on the FBMC scheme. For example, for Staggered Multitone (SMT) such a symbol period is $T_{\text{SMT}} = T_s N_c/2$.

As proposed in our previous work [11], the parameter T can be adjusted by time interpolation by a factor I, yielding an FBMC symbol period $T^{(I)} = IT$, and consequently an I times narrower signal bandwidth (see Fig. 1), which leads to a reduced subcarrier spacing (also by a factor of I). Therefore, given the actual velocity v of the mobile receiver, the normalized Doppler spread, impacting the time-interpolated FBMC signal can be written as

$$D_n^{(I)} = f_d T^{(I)} = f_d I T = \frac{I T f_c v}{c} = \frac{T f_c}{c} v^{(I)}, \qquad (2)$$

with f_c the carrier frequency, c the speed of light, and $v^{(I)} = Iv$ the emulated speed as a result of an actual measurement speed v and an interpolation factor I. Consequently, enlarging the symbol period $T^{(I)}$ by adjusting I allows for the emulation of a velocity $v^{(I)}$ while conducting measurements at a (presumably much lower) speed v.

In our setup, time-interpolation factors $I = 1, 2, 3$ were applied to FBMC signals to emulate I times higher velocities than the actual speed used to configure the channel model. More specifically, an FBMC system using Offset QAM (OQAM) symbols, the so-called SMT architecture [1], was considered.

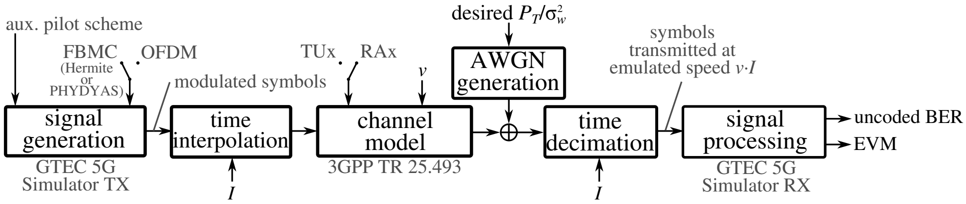

Fig. 2. Block diagram of the setup used for the evaluations.

III. Evaluation Setup

We use the evaluation setup shown in Fig. 2 to test the technique of emulating high speeds by time interpolation of FBMC signals. The setup consists of the blocks explained below.

A. Signal Generation and Signal Processing

At the transmitter side, FBMC-modulated signals are generated by using a custom-developed FBMC signal generator. Two different pulses were implemented, namely the one defined by the PHYDYAS project [13] and the so-called Hermite pulse [5]. It is worth noting that the latter one is specially suited for multicarrier transmissions over doubly dispersive channels since it minimizes both the ICI and Inter-Symbol Interference (ISI) by means of a good localization in time and frequency [5]. Our signal generator also supports OFDM signals (which correspond to the use of a rectangular filter in the time domain). At the receiver side, a custom-developed FBMC receiver is used. Such a receiver includes:

- **Basic channel estimation**: the channel response is estimated by means of a grid of pilots. For the case of FBMC signals, the receiver has to deal with the interference caused by the lack of orthogonality of the received signal, since only orthogonality in the real part is assured [1]. Several methods that minimize the effect of the interference based on the so-called auxiliary pilot schemes were implemented [14]–[16]. For the results shown in this paper, the so-called Coded Auxiliary Pilot (CAP) method [16] (using 8 symbols around each pilot) was considered.
- **Basic channel interpolation**: two-dimensional (time and frequency) interpolation techniques are used. More specifically, an interpolator based on the use of cubic splines is used.
- **Basic channel equalization**: a basic Zero-Forcing (ZF) equalizer was implemented.

Time and frequency synchronization algorithms are also implemented. However, in order to avoid distorting the results shown in this paper, perfect time and frequency synchronization was considered.

Finally, figures of merit such as the uncoded Bit Error Ratio (BER) and the Error Vector Magnitude (EVM) (see Section IV) are estimated at the receiver.

B. Time Interpolation and Time Decimation

The signal is time-interpolated by a factor I at the transmitter and decimated by the same factor I at the receiver side. This way we emulate a Doppler spread similar to that obtained with a speed increase by a factor of I (see Section II).

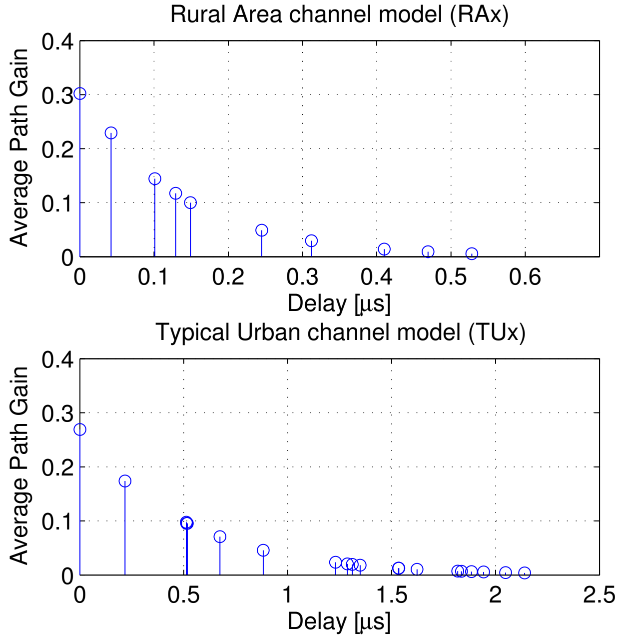

Fig. 3. Power Delay Profile of the considered channel models (Rural Area channel model and Typical Urban channel model).

C. Channel Model

We evaluate, by means of simulations, the technique of emulating high speeds by time interpolation. We select noise variance values that lead to the desired P_T/σ_w^2 values, where P_T and σ_w^2 denote the transmitted power and the noise variance, respectively. Two channel models were considered in order to evaluate the performance of the velocity emulation technique for various scenarios. More specifically, the profiles Rural Area channel model (RAx) and Typical Urban channel model (TUx) of the 3rd Generation Partnership Project (3GPP) channel models for deployment evaluation [17] were considered. The Doppler spread parameter of the channel was set according to the desired speed and carrier frequency values. While the profile RAx models the typical scenario in which a train moves across a rural area covered by macro-cells, the TUx environment is more suitable for situations in which the train moves through urban areas.

The Power Delay Profile (PDP) of the considered channel models is shown in Fig. 3.

TABLE I
COMBINATIONS OF VELOCITIES AND INTERPOLATION FACTORS WHICH LEAD TO EQUAL DOPPLER SPREADS.

Emulated velocity	$I = 1$	$I = 2$	$I = 3$
100 km/h	$v = 100$ km/h	$v = 50$ km/h	–
200 km/h	$v = 200$ km/h	$v = 100$ km/h	$v = 66.6$ km/h
300 km/h	$v = 300$ km/h	$v = 150$ km/h	$v = 100$ km/h
400 km/h	$v = 400$ km/h	$v = 200$ km/h	$v = 133.3$ km/h

IV. EVALUATION PROCEDURE

In order to evaluate the impact of high-speed conditions on FBMC transmissions, actual velocities ranging from 50 km/h to 400 km/h were considered for the channel models. Furthermore, interpolation factors of $I = 1$ (no interpolation), $I = 2$, and $I = 3$ were used for generating Doppler spreads equivalent to those associated to velocities ranging from 50 km/h to 1200 km/h. Note that it is possible to generate exactly the same Doppler spread value from different combinations of the actual velocity (the one used to configure the channel model) and the interpolation factor (see Table I). This fact is helpful to show that our technique allows for the evaluation of wireless communication systems at high speeds while measuring at much lower speeds. In order to do that, we generated the same Doppler spread by means of different velocities and interpolation factors and then we compared the obtained results. Table I shows the combinations of actual speeds and interpolation factors which lead to equal Doppler spreads (each row of the table corresponds to a different Doppler spread factor).

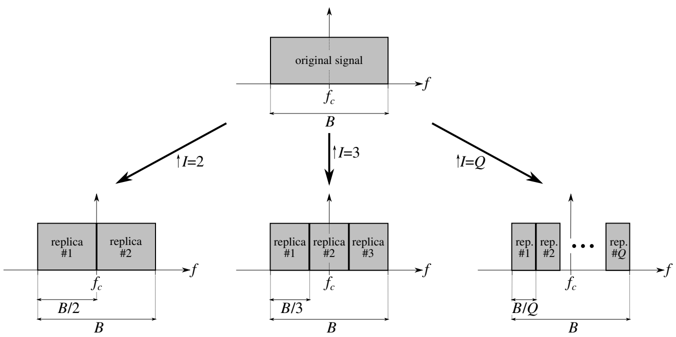

Fig. 4. Ensuring equal spectrum usage for interpolation factors $I = 2, 3$ and for an arbitrary integer interpolation factor $I = Q$. I replicas of the interpolated signal are transmitted to ensure that the whole frequency range of the original signal (without interpolation) is used. In this figure the signal bandwidth is denoted by B.

To be able to compare the results gathered from different interpolation factors and the distinct modulations considered, the following aspects are taken into account.

A. Equal Mobile Simulated Trajectory

To fairly compare the results, the channel model was generated with identical initial conditions and the same seed (for the pseudo-random numbers generator) for each evaluated velocity and interpolation factor values. This way, we model a situation in which the receiver moves along the same path for each interpolation factor.

B. Equal Spectrum Usage

When the signal is interpolated by a factor of I, its bandwidth is decreased by the same factor, which in principle reduces the frequency diversity of the channel. In order to experience the same spectrum, I replicas of the interpolated signal are transmitted to ensure that the whole frequency range of the original signal is used. The results are then averaged. Figure 4 shows an example of this procedure for $I = 2$.

C. Equal Average Transmit Energy per Symbol

In order to preserve the average energy per symbol, the interpolated signals are scaled in amplitude by a factor of $\sqrt{I}$ before being transmitted.

D. Ensuring a Fair OFDM vs FBMC Comparison

In order to be able to fairly compare the results for the different considered modulations (OFDM and FBMC with Hermite and PHYDYAS pulses), the following aspects were also considered:

- The number of data subcarriers, as well as the subcarrier spacing, are the same in all cases. More specifically, 600 subcarriers are used, while the subcarrier spacing was set to 15 kHz (for the OFDM case, 600 subcarriers are used for a 1024-point Fast Fourier Transform (FFT)). These parameters correspond to the typical configuration for the 10 MHz downlink LTE profile.
- The pilot density considered for channel estimation is equivalent in all cases. Note that in the case of FBMC some additional symbols, namely the Auxiliary Pilots (APs), are required to minimize the interference caused by the lack of orthogonality of the received pilots [1]. More specifically, a rectangular grid of pilots was used. Such pilot spacing in the time-frequency grid is of 8 subcarriers in the frequency dimension and of 10 symbols in the time dimension for SMT signals (5 symbols in the case of OFDM given that consecutive symbols do not overlap).
- The same algorithms for channel estimation, interpolation and equalization are considered for each of the modulations (see Section III).
- A 2-PAM constellation is used for the FBMC transmissions, while 4-QAM is considered for OFDM, since the symbols are complex-valued in the latter case.
- Approximately the same number of user data bits is considered per transmission. Taking into account that real-valued symbols are used in FBMC, whereas complex-valued ones are used for OFDM, more time-positions in the time-frequency grid are required for FBMC signals with respect to OFDM for the same number of transmitted bits. However, provided that consecutive FBMC symbols partially overlap in the time domain (because a SMT scheme is considered), this does not mean that in order to transmit the same amount of data bits we need twice the

time-positions for FBMC with respect to OFDM. With the model considered, the user bit rate is approximately equivalent for both OFDM and FBMC, with slight differences caused by the length of the OFDM cyclic prefix and the time dispersion of the prototype filters in FBMC.
- The signals are scaled to ensure that the transmitted energy per bit is equivalent for both OFDM and FBMC.

Note that the number of used subcarrriers could be increased in FBMC with respect to OFDM for a common spectral mask, as the subcarriers are better frequency-localized. Futhermore, we could also increase the bandwidth per subcarrier, i.e., decrease the number of subcarriers while keeping the total used bandwidth constant, for FBMC. Although this would require more advanced equalizers, it will be beneficial in terms of Peak-to-Average Power Ratio (PAPR). However, to perform a more fair comparison, we decided to keep both the number of subcarriers as well as the subcarrier spacing constant, although this would imply not to take advantage of all the potencial benefits of FBMC systems. This enables us to consider an approximately equivalent number of user data bits per transmission for the FBMC and the OFDM cases, while the same algorithms for channel estimation, interpolation and equalization are also employed, as mentioned before.

We consider two figures of merit for the results, which are:
- **EVM**: it is calculated assuming the transmitted symbols are known beforehand. It is an unbounded and continuous metric particularly valuable when the Signal-to-Noise Ratio (SNR) is high enough to saturate the BER to its minimum value of zero. In order to compute the EVM, the dynamic range of the equalized symbols is bounded. This is realistic in a practical receiver. In this sense, real and imaginary parts of the symbols are clipped to a maximum value. This avoids symbols having extremely large modulus (e.g., due to imperfect ZF channel equalization), hence distorting the EVM estimation. It is worth mentioning that, for the case of FBMC, only the real part of the symbols is considered to compute the EVM, since the imaginary part contains the interference generated by the lack of orthogonality of the signals [1] and it is ignored by the receiver.
- **Uncoded BER**: calculated as the BER after the hard symbol decision. It is one of the most used performance metrics in wireless communications.

Table II details the most relevant parameters considered in the experiments.

TABLE II
MAIN PARAMETERS USED IN THE EXPERIMENTS.

parameter	**value**
Sampling frequency, F_s	15.36 MHz
FFT size	1024
Number of used subcarriers	600 (excluding DC)
CP length (OFDM)	72 samples
Constellations	2-PAM (FBMC) 4-QAM (OFDM)
Pilot spacing	8 subcarriers (frequency dimension) 10 symbols (time dimension, FBMC) 5 symbols (time dimension, OFDM)
AP scheme	CAP (8 surrounding symbols)
Pulse overlapping	3 symbols (Hermite) 4 symbols (PHYDYAS)
Velocities, v	50, 66.6, 100, 133.3, 150, 200, 300, and 400 km/h
Carrier frequency, f_c	2.6 GHz
Interpolation factors, I	1, 2, and 3
P_T/σ_w^2	0, 5, 10, 15, 20, 25, and 30 dB

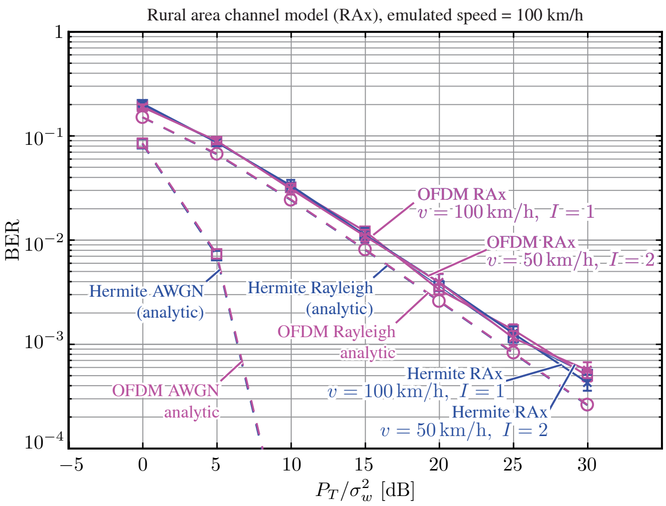

Fig. 5. BER versus P_T/σ_w^2 for the RAx channel model.

V. Results

All the results included in this section are expressed in terms of BER and EVM with respect to the P_T/σ_w^2, and with respect to the so-called "emulated speed", which means that the speed can correspond to the actual velocity ($I = 1$) or a velocity obtained by time-interpolating the transmit signal. With the objective of gauging the accuracy of the results, 95 % confidence intervals are also included.

Figure 5 shows the BER versus P_T/σ_w^2 for the RAx channel model when an emulated speed of 100 km/h is obtained considering $I = 1$ (no interpolation) and $I = 2$, for the cases of OFDM and FBMC (Hermite prototype filter). Analytic curves for both Additive White Gaussian Noise (AWGN) and Rayleigh channels for the cases of OFDM and FBMC are also included. It can be seen that such analytic curves overlap, ensuring that a fair comparison is performed. With respect to the simulation results, the curves corresponding to OFDM for the emulated speed $v = 100$ km/h obtained by considering the interpolations factors $I = 1$ and $I = 2$ almost overlap. The same effect can be appreciated for the curves corresponding to FBMC. Moreover, there is an excellent agreement between the OFDM and FBMC results for most P_T/σ_w^2 values. This shows that the performance of both modulation schemes is very similar for $v = 100$ km/h and the RAx channel model. Only slight differences are appreciated for the maximum P_T/σ_w^2

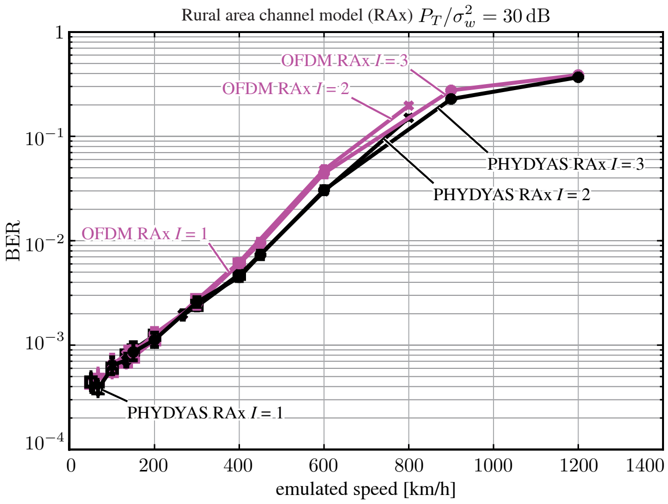

Fig. 6. BER versus emulated speed for OFDM and FBMC with the PHYDYAS prototype filter. RAx channel model and $P_T/\sigma_w^2 = 30\,\text{dB}$.

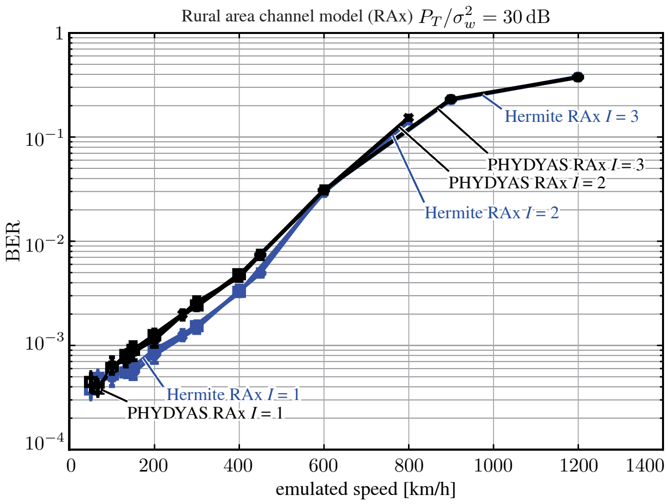

Fig. 7. BER versus emulated speed for FBMC with the PHYDYAS and Hermite prototype filters. RAx channel model and $P_T/\sigma_w^2 = 30\,\text{dB}$.

value of 30 dB, since the random effects due to the noise are minimized and hence do not hide the other sources of disagreement in the results. Therefore, in the remaining result figures we consider $P_T/\sigma_w^2 = 30\,\text{dB}$ as the worst case for the proposed technique.

Figure 6 shows the BER versus the emulated speed for the RAx channel model and considering OFDM and FBMC with the PHYDYAS prototype filter. All interpolation factors $I = 1, 2, 3$ are considered. On the one hand, the three OFDM curves corresponding to the three interpolation factors show an excellent level of agreement. The same effect is appreciated for the FBMC (PHYDYAS) curves. On the other hand, a significant performance difference between OFDM and FBMC (PHYDYAS) is appreciated for speeds above 300 km/h. This is because the PHYDYAS prototype filter is much better localized in frequency than the OFDM one, and hence accounting

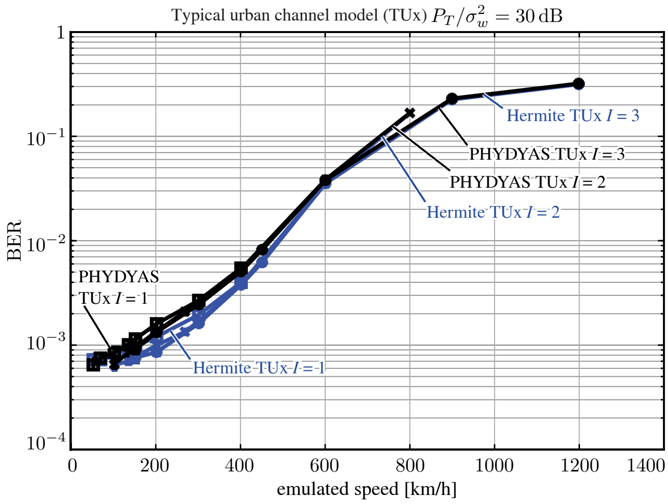

Fig. 8. BER versus emulated speed for the TUx channel model and $P_T/\sigma_w^2 = 30\,\text{dB}$.

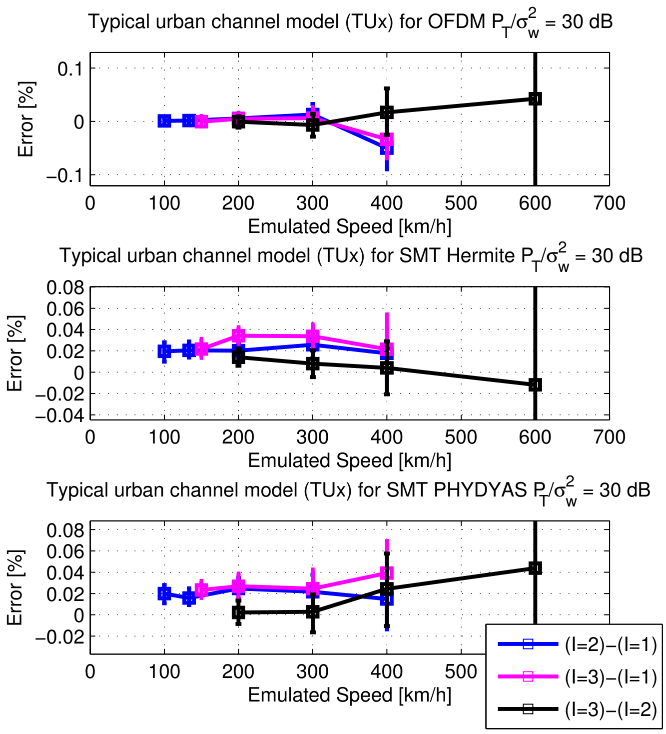

Fig. 9. Relative error curves for BER evaluations over the TUx channel model. An excellent agreement can be appreciated. Notice that the confidence interval for the case labeled as "$(I = 3)$ - $(I = 2)$" is not completely shown in the graphs. The lower bounds of such an interval are approximately $-0.43\,\%$, $-0.24\,\%$ and -0.24% for the OFDM, SMT (Hermite) and SMT (PHYDYAS) cases, respectively. The respective upper bounds of the confidence interval are approximately $0.39\,\%$, $0.24\,\%$ and $0.23\,\%$.

better for the channel time dispersion. In other words, the FBMC PHYDYAS prototype filter helps in combating the effect of the ICI better than OFDM. However, for practical HST velocities (around 300 km/h) the performance difference

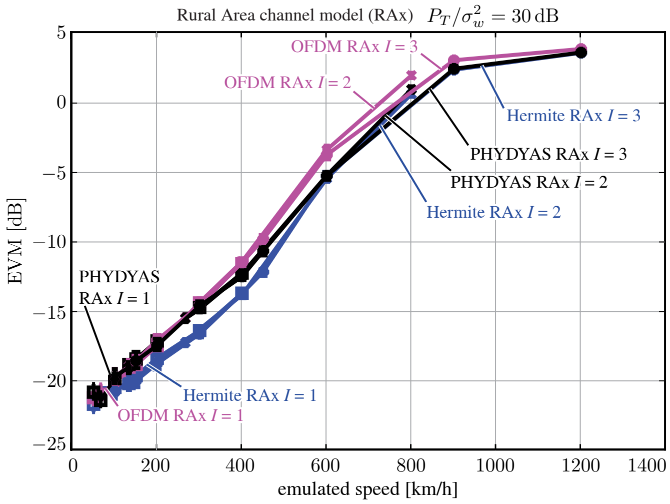

Fig. 10. EVM versus emulated speed for the RAx channel model and $P_T/\sigma_w^2 = 30\,\mathrm{dB}$.

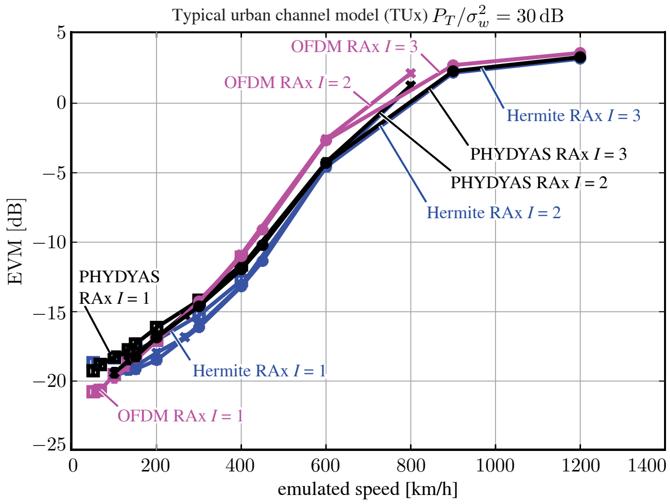

Fig. 11. EVM versus emulated speed for the TUx channel model and $P_T/\sigma_w^2 = 30\,\mathrm{dB}$.

is not very significant.

Figure 7 shows the same information as Fig. 6 but only for the two FBMC prototype filters considered (Hermite and PHYDYAS). Again, an excellent agreement is shown between the emulated speeds obtained by means of different interpolation factor regardless of the considered scheme. Figure 7 also shows that the performance obtained with the Hermite prototype filter is better than that exhibited by the PHYDYAS one, specially for those speeds which are more practical in the HST environment. The reason for this behavior is because the Hermite prototype filter is slightly worse localized in frequency than the PHYDYAS one, but it is better localized in time, thus simultaneously minimizing both ICI and ISI.

Figure 8 presents again the same results but considering the TUx channel model. Given that the TUx channel model is more frequency selective than the RAx one, the BER values

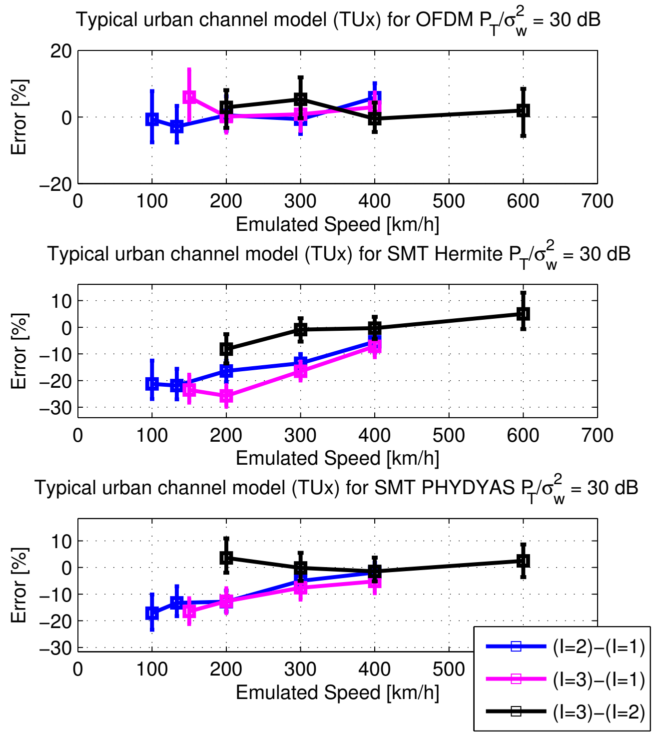

Fig. 12. Relative error curves for EVM evaluations over the TUx channel model. An excellent agreement can be appreciated.

are worse than those obtained for the RAx. On the other hand, the level of agreement between the curves corresponding to the three interpolation factors is also slightly worse than in the RAx case, specially between the curves for $I = 1$ and the others, and for speeds below 300 km/h.

Besides the performance curves, we have also included in Fig. 9 the BER relative error curves for the worst case (TUx channel model). Three types of relative error curves are included, which are *(a)* relative difference between the results obtained when the interpolation factor $I = 2$ is employed and actual speeds are used; *(b)* relative difference between the results obtained when the interpolation factor $I = 3$ and the actual speeds are considered; and *(c)* relative difference between the results obtained for the interpolation factors $I = 3$ and $I = 2$. The relative error is computed by averaging the instantaneous BER relative error values E_{BER}, which are computed as

$$E_{\mathrm{BER}}(A, B) = 100 \cdot \frac{W_A - W_B}{W_B}\ [\%],$$

where W_A and W_B denote the number of received bits estimated without errors, corresponding to a channel realization and obtained for the interpolation factors $I = A$ and $I = B$, respectively. Together with the mean values, we provide the corresponding 95% bootstrap confidence intervals. The magnitude of the mean values of the BER relative error is below $0.05\,\%$ for all the scenarios and velocities considered, which confirms the good behavior of the proposed technique.

The performance in terms of EVM versus emulated speed is shown in Fig. 10 for the RAx channel model, and in Fig. 11 for the TUx channel model. These results are in accordance with those obtained for the BER. Again, an excellent level of agreement between the curves obtained for different interpolation factors can be appreciated, thus validating the proposed technique for inducing high-speed effects while evaluating the system under test at much lower velocities.

In Fig. 12 the EVM relative error curves for the worst case (TUx channel model) were included. In this case, they are computed by averaging the instantaneous EVM relative error values, which are computed as

$$E_{\mathrm{EVM}}\left(A,B\right) = 100 \cdot \frac{\mathrm{EVM}_A - \mathrm{EVM}_B}{\mathrm{EVM}_B}\ [\%]\,,$$

where EVM_A and EVM_B are the instantaneous EVM values for the interpolation factors $I = A$ and $I = B$, respectively. We gauge the precision of the error estimates by calculating the 95% confidence intervals for the mean. The magnitude of the mean values of the EVM relative error is below $25\,\%$ for all the scenarios and velocities considered.

VI. Conclusions

In this work we have proposed a technique to induce the effects caused by highly time-varying wireless channels in FBMC-modulated signals while conducting the measurements (or the evaluations) at much lower velocities. This allows for reducing the complexity, cost, and safety constraints of measurement campaigns in HST scenarios. The proposed technique was evaluated both in terms of BER and EVM and considering two FBMC prototype filters: the one proposed in the context of the PHYDYAS project and the so-called Hermite pulse.

The obtained performance results were also compared to those exhibited by OFDM. It was shown that for high speeds (exceeding 300 km/h), FBMC can be a much better choice than OFDM, specially when well localized prototype filters, both in time and in frequency, are employed, e.g. the Hermite pulse. However, for practical HST velocities (around 300 km/h) the performance difference is not very significant.

In this work we considered an isolated point-to-point link which does not exploit all the potential advantages of the FBMC schemes, mainly their better bandwidth efficiency. Such a bandwidth efficiency is very important for the coexistence between current GSM-R and the new broadband wireless systems as well as to avoid multiple-access interference in the uplink. The obtained results confirm that FBMC advantages can be exploited in HST environments without additional performance losses.

Finally, from the excellent agreement of the results obtained from the simulations for the considered figures of merit (BER and EVM) and regardless actual or emulated speeds, it can be concluded that the proposed technique is valid for inducing high-speed effects in FBMC-based systems.

Acknowledgment

This work has been funded by Xunta de Galicia, MINECO of Spain, and FEDER funds of the EU under grants with numbers 2012/287, TEC2013-47141-C4-1-R, FPU12/04139, EST14/00355, and BES-2014-069772.

The authors thank the Institute of Telecommunications at the TU Wien, Vienna, Austria, and specially Markus Rupp.

References

[1] B. Farhang-Boroujeny, "Ofdm versus filter bank multicarrier," *Signal Processing Magazine, IEEE*, vol. 28, no. 3, pp. 92–112, 2011.

[2] M. Morelli, C. J. Kuo, and M.-O. Pun, "Synchronization techniques for orthogonal frequency division multiple access (ofdma): A tutorial review," *Proceedings of the IEEE*, vol. 95, no. 7, pp. 1394–1427, 2007.

[3] B. L. Floch, M. Alard, and C. Berrou, "Coded orthogonal frequency division multiplex [tv broadcasting]," *Proceedings of the IEEE*, vol. 83, no. 6, pp. 982–996, 1995.

[4] M. Alard, "Construction of a multicarrier signal," Aug. 21 2001, uS Patent 6,278,686.

[5] R. Haas and J.-C. Belfiore, "A time-frequency well-localized pulse for multiple carrier transmission," *Wireless Personal Communications*, vol. 5, no. 1, pp. 1–18, 1997.

[6] T. Strohmer and S. Beaver, "Optimal ofdm design for time-frequency dispersive channels," *Communications, IEEE Transactions on*, vol. 51, no. 7, pp. 1111–1122, 2003.

[7] P. Amini, C. H. Yuen, R.-R. Chen, and B. Farhang-Boroujeny, "Isotropic filter design for mimo filter bank multicarrier communications," in *Sensor Array and Multichannel Signal Processing Workshop (SAM), 2010 IEEE*. IEEE, 2010, pp. 89–92.

[8] J. Rodríguez-Piñeiro, M. Lerch, J. A. García-Naya, S. Caban, M. Rupp, and L. Castedo, "Emulating extreme velocities of mobile LTE receivers in the downlink," *EURASIP Journal on Wireless Communications and Networking*, vol. 2015, no. 106, April 2015, special Issue on Experimental Evaluation in Wireless Communications. Online access: http://dx.doi.org/10.1186/s13638-015-0343-0.

[9] J. Rodríguez-Piñeiro, M. Lerch, P. Suárez-Casal, J. A. García-Naya, S. Caban, M. Rupp, and L. Castedo, "LTE downlink performance in high speed trains," in *2015 IEEE 81st Vehicular Technology Conference (VTC2015-Spring)*, Glasgow, United Kingdom, May 2015, accepted for publication.

[10] J. Rodríguez-Piñeiro, J. A. García-Naya, A. Carro-Lagoa, and L. Castedo, "A testbed for evaluating LTE in high-speed trains," in *2013 Euromicro Conference on Digital System Design*, Sept 2013, pp. 175–182.

[11] J. Rodríguez-Piñeiro, P. Suárez-Casal, J. A. García-Naya, L. Castedo, C. Briso-Rodríguez, and J. I. Alonso-Montes, "Experimental validation of ICI-aware OFDM receivers under time-varying conditions," in *IEEE 8th Sensor Array and Multichannel Signal Processing Workshop (SAM 2014)*, A Coruña, Spain, June 2014.

[12] P. Suárez-Casal, J. Rodríguez-Piñeiro, J. A. García-Naya, L. Castedo, C. Briso-Rodríguez, and J. I. Alonso-Montes, "Experimental assessment of WiMAX transmissions under highly time-varying channels," in *Eleventh International Symposium on Wireless Communication Systems (ISWCS)*, Barcelona, Spain, August 2014, pp. 717–721, online access: http://dx.doi.org/10.1109/ISWCS.2014.6933447.

[13] M. Bellanger, D. Le Ruyet, D. Roviras, M. Terré, J. Nossek, L. Baltar, Q. Bai, D. Waldhauser, M. Renfors, T. Ihalainen *et al.*, "Fbmc physical layer: a primer," PHYDYAS FP7 Project Document, Tech. Rep., 2010.

[14] J.-P. Javaudin, D. Lacroix, and A. Rouxel, "Pilot-aided channel estimation for ofdm/oqam," in *Vehicular Technology Conference, 2003. VTC 2003-Spring. The 57th IEEE Semiannual*, vol. 3. IEEE, 2003, pp. 1581–1585.

[15] T. H. Stitz, T. Ihalainen, A. Viholainen, and M. Renfors, "Pilot-based synchronization and equalization in filter bank multicarrier communications," *EURASIP Journal on Advances in Signal Processing*, vol. 2010, p. 9, 2010.

[16] W. Cui, D. Qu, T. Jiang, and B. Farhang-Boroujeny, "Coded auxiliary pilots for channel estimation in FBMC-OQAM systems," *IEEE Transactions on Vehicular Technology*, vol. PP, no. 99, pp. 1–1, 2015.

[17] 3GPP, "3GPP TR 25.943: 3GPP; Technical specification group radio access network; Univerlsal Mobile Telecommunications System (UMTS); Deployment aspects," ETSI, Tech. Rep., December 2004.